

# An Integrated Frequency-Voltage Controller for Next-Generation Power Systems

Etinosa Ekomwenrenren<sup>a</sup>, Zhiyuan Tang<sup>a</sup>, John W. Simpson-Porco<sup>b</sup>, Evangelos Farantatos<sup>c</sup>,  
Mahendra Patel<sup>c</sup>, Hossein Hooshyar<sup>c</sup>, Aboutaleb Haddadi<sup>c</sup>

<sup>a</sup>Department of Electrical and Computer Engineering, University of Waterloo, Waterloo, ON N3L 3G1 CA

<sup>b</sup>Department of Electrical and Computer Engineering, University of Toronto, Toronto, ON, M5S 3G4, CA

<sup>c</sup> Electric Power Research Institute, Palo Alto, CA 94304 USA

**Abstract**—This paper presents an integrated frequency-voltage controller design for next-generation power systems. The approach is built on our previous work, where we designed frequency and voltage controllers for the coordinated control of fast-acting inverter-based resources (IBRs) and other legacy sources of power supply in IBR-dominated grids. Here, we integrate these controllers into a joint frequency-voltage control framework. This integration allows the independently designed frequency and voltage control strategies to both utilize the IBRs simultaneously to provide the requisite control services, while also addressing a myriad of integration issues. The joint action of the frequency and voltage controllers under our proposed integration is illustrated via several case studies.

**Index Terms**—renewable energy, voltage control, frequency control, transmission grid, smart grid

## I. INTRODUCTION

The penetration of inverter-connected renewable energy resources (RESs) is increasing in the transmission grid [1]. This change brings new challenges to the classical problems of transmission system frequency and voltage control. The reduction in the system rotational inertia, due to the increased proliferation of inverter-based resources (IBRs), can impact power system stability and operation, resulting in large frequency deviations, faster frequency dynamics and increased net load variability in the system [1], [2]. On the voltage control side, challenges include (but are not limited to) increased voltage fluctuations and voltage limit violations, cascading outages, and voltage stability issues such as fault-induced delayed voltage recovery (FIDVR) [3], [4].

The development of new control methods is required to address these challenges, and has been the subject of investigation of our previous works [5], [6]. There, we designed a frequency controller (FC) and a voltage controller (VC) for the control and coordination of fast-acting IBRs and other legacy sources of power supply in next-generation grids. These controllers allows for the quick and accurate correction of active and reactive power imbalances arising in the system, thereby minimizing frequency and voltage deviations. Both controllers have been extensively validated via case studies. We provide a brief overview of these schemes in the Section II.

This paper proposes an integration of the previously developed controllers into a joint frequency-voltage control

framework, which enables IBRs to simultaneously participate in both frequency and voltage control in a coordinated fashion. Depending on the system conditions and operator preferences, the available capacity of the IBRs must be allocated in a principled fashion between these two control schemes, which will otherwise vie for the same resources; here we examine the relative advantages and disadvantages of different priority allocation schemes. Additionally, we examine frequency-voltage cross-couplings in the system — such as voltage-dependent consumption of loads and the action of power-system stabilizers through the excitation systems of synchronous generators (SGs) — that can impact the performance of the joint frequency-voltage control scheme, and provide recommendations for how to minimize these couplings.

The remainder of this paper is organized as follows. Section II provides a review of the novel frequency and voltage control schemes, which are to be integrated in this work. In Section III, we outline the technical approach, before presenting simulation results in Section IV. Section V concludes the report and outlines future research directions.

## II. REVIEW OF HIERARCHICAL FREQUENCY AND VOLTAGE CONTROL SCHEMES

### A. Frequency Control Scheme

Reference [5] has presented the details of the FC, which is a hierarchical two-layer IBR control scheme for fast and localized frequency control in next-generation grids. The key principle is to partition the power system into small (e.g., several substations) local control areas (LCAs), and use IBRs in each LCA to provide fast and localized response to frequency events, such as a large load disturbance and/or generation outage. For each LCA, a local disturbance estimator computes a running estimate of active power imbalance within the area. Using this estimate, a local control loop quickly redispatches local IBRs to balance local generation and net load. The design of the local control loop is based on the classical internal model control (IMC) structure [7]. In situations where the local IBR resources are insufficient to restore power balance, additional power support is optimally sourced from neighboring areas; this can be mediated by a central coordinating controller, or achieved in a privacy-preserving distributed fashion.

Funded under EPRI Project #10009168: Wide-Area Hierarchical Frequency and Voltage Control for Next Generation Transmission Grids.

## B. Voltage Control Scheme

Reference [6] has presented the details of the VC, which mitigates voltage violations in the grid due to unmeasured disturbances. In the proposed method, reactive power injections of fast-acting IBRs and other traditional voltage control devices (such as synchronous generators (SGs) and static var compensators (SVCs)) are coordinated to maintain grid voltages within desired limits. The scheme capitalizes on recent advances in wide-area communication and monitoring by using real-time measurement-based feedback control. The scheme requires minimal model information, is highly amenable to fast online implementation, and is robust against modelling error and changing grid conditions.

## III. JOINT FREQUENCY-VOLTAGE CONTROL INTEGRATION

Fig. 1 presents a diagram of the developed joint frequency-voltage (F-V) control framework. This framework integrates the previously developed FC and VC, allowing the two controllers to operate simultaneously despite relying on the same IBRs as the key resources for providing their control services. The main issues of relevance when integrating the controllers are (i) IBR capacity allocation, (ii) voltage-frequency interactions, and (iii) VC-PSS interactions. We now investigate the nature of these interactions, and provide solutions for mitigating the resulting integration challenges.

### A. Capacity Allocation and Operation Modes

Since both the FC and VC make use of IBR resources within each control area, the allocation of IBR capacity between the controllers is a key consideration. We consider two possible modes of operation, one where the FC has capacity priority, denoted  $FC > VC$ , and one where the VC has capacity priority, denoted  $VC > FC$ . Let  $(P^*, Q^*)$  denote the current dispatch point for the IBR, with  $S_r$  its apparent power rating. When the FC has control priority, it selects the desired active power, and any remaining capacity is made available to the VC. Specifically, at time  $t$  the allocation procedure is

$$P(t) \in [0, \sqrt{S_r^2 - (Q^*)^2}] \quad (1a)$$

$$Q(t) \in [-\sqrt{S_r^2 - P(t)^2}, \sqrt{S_r^2 - P(t)^2}]. \quad (1b)$$

Note that (2a) ensures that the IBR can continue to meet its dispatched reactive power value. When the VC has control priority, the priority allocation principle above is reversed:

$$Q(t) \in [-\sqrt{S_r^2 - (P^*)^2}, \sqrt{S_r^2 - (P^*)^2}] \quad (2a)$$

$$P(t) \in [0, \sqrt{S_r^2 - Q(t)^2}]. \quad (2b)$$

Selecting the control priority depends on the system configuration and the operator preferences. However, given that voltage is local and frequency support can be sought more easily from other interconnected areas, the mode  $VC > FC$  would typically be preferred except when stringent frequency control is required.

## B. Interaction due to Voltage-Sensitivity Loads

An interaction between the two controllers arises due to voltage-dependent power consumption of (e.g., impedance-type) loads. The interaction mechanism is as follows. As the voltage controller acts to regulate voltage levels, the active power consumption of voltage-sensitive loads changes. The disturbance estimator embedded within the frequency controller interprets this change as a load imbalance, and adjusts IBR power levels to compensate. Finally, the resulting frequency swings are fed back to the AVR system via any PSS action, completing the feedback loop. These interactions between disturbance estimator, voltage controller, and PSS action may lead to oscillations in some edge cases.

This effect can be compensated by embedding a crude load model within the frequency controller. To this end, consider a standard impedance load model [8] and its linearization

$$P_{\text{load}} = P_0 \left( \frac{V}{V_0} \right)^2 \quad \implies \quad \Delta P_{\text{load}} = \frac{2P_0}{V_0} \Delta V.$$

The change in loading  $\Delta P_{\text{load}}$  can be computed using real-time voltage measurements<sup>1</sup>. The result  $\Delta P_{\text{load}}$  is passed through a washout filter  $\frac{s}{s+\omega_0}$ , and is then provided to the disturbance estimator within the frequency controller [5]. The washout filter ensures that the frequency controller does indeed compensate for *steady-state* loading changes arising from the post-disturbance operating point. Tuning of the cut-off frequency  $\omega_0$  is a straightforward trade-off between transient decoupling and the speed of frequency regulation.

### C. VC-PSS Interactions

Another interaction can occur between the VC and any PSS systems which are implemented at SGs. For SGs, the VC operates by providing a modified reference voltage to the AVR system. However, PSS controllers also make use of the generator excitation system to damp frequency oscillations; these two signals have the potential to oppose each other at the input to the SG excitation system. This is most pronounced in the case of multiband power system stabilizers [9] that are used to damp global oscillations, which are typically under 0.2 Hz. A simple way to address this conflict is to restrict the signal sent by the VC to the SGs to have an even lower bandwidth than the PSS operating frequency range, so that it does not interfere with the PSS signal. This is accomplished by low-pass filtering the voltage reference signal with a sufficiently large time constant. However, in the case of the multiband PSS, the frequency range of interest is already quite low; a practical solution in this case would be to simply remove the SG from the VC scheme. This interaction will be illustrated in Fig. 8 in Section IV-B.

## IV. SIMULATION STUDIES

The single-line diagram of a three-area test system is shown in Figure 2, where each of the individual one-area systems is

<sup>1</sup>We note that since the voltage controller is assumed to receive either voltage measurements or estimates thereof, there is no additional assumption in using the voltage measurements in this compensation scheme.

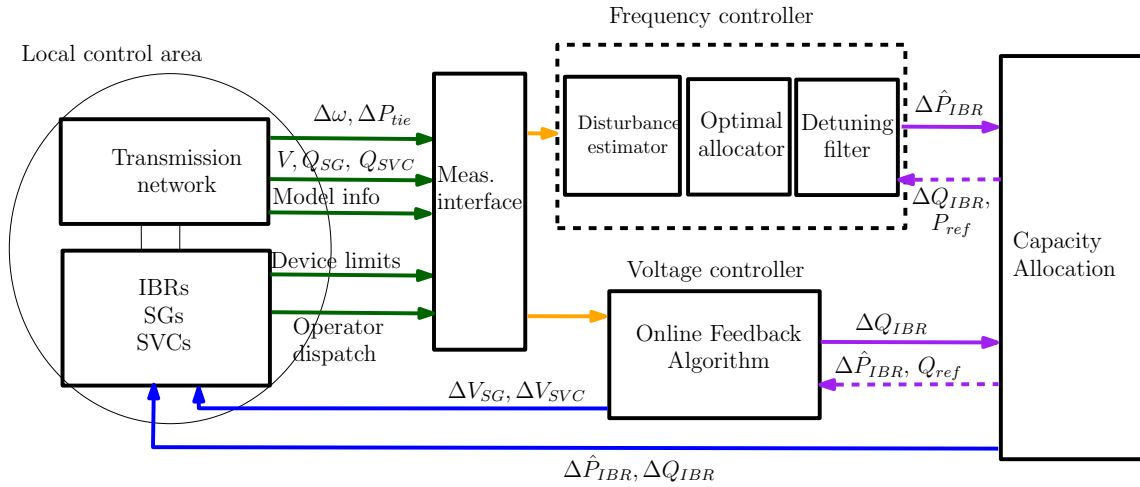


Fig. 1. Schematic illustration of joint F-V control framework.

modified based on the IEEE 3-machine 9-bus system [10]. In the modified model, two IBRs and one SVC are added to areas 1 and 2, while two SGs in area 3 are replaced with two IBRs with the same capacities.

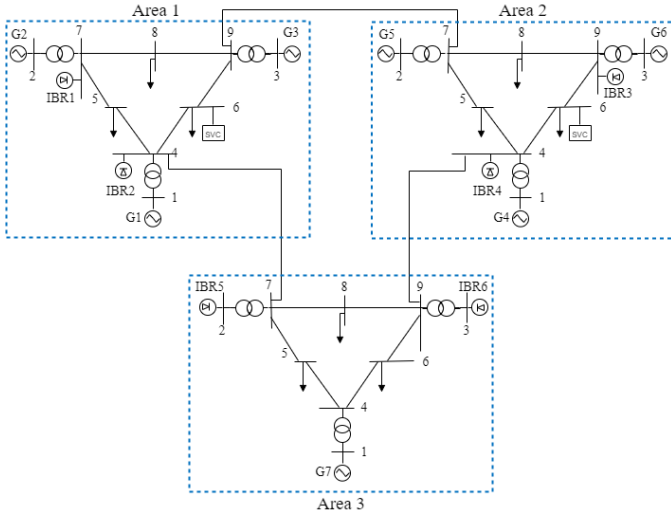


Fig. 2. Three-area test system.

We consider here two scenarios to illustrate the basic functionality in the proposed F-V control framework: (i) a large step load change in one area, but where the active power demand can be fully compensated with only local resources, and (ii) a larger step load change in the same LCA, where active power support from the other areas will be required. The magnitudes and power factors of load disturbances introduced in both scenarios are exaggerated in order to more clearly assess the performance of the control framework. For the scenarios considered, the IBRs are the only devices available for active power redistribution, and are also the preferred reactive power resources for voltage regulation (the latter is a design setting within the voltage controller; see [6] for details).

### A. Scenario # 1: load disturbance

This scenario illustrates the basic performance of the controller when operating in the VC priority mode. A large load disturbance of 70 MW and 100 Mvar occurs at  $t = 1$  s at bus 8 in Area 3. The response of the system is shown in Fig. 3, 4, 5. Here, dotted and solid lines refer to cases without and with control, respectively; the dashed line refers to the capacity limit of each IBR. We can observe from Fig. 3 and 4 that the frequency can be restored to its nominal value quickly while the voltage levels are kept within the limits in steady-state, in contrast to the case with no control. Note from Fig. 3, that the device active/reactive power outputs in the *non-contingent* areas are kept close to their initial points in steady-state; put differently, control response is localized to the contingent area.

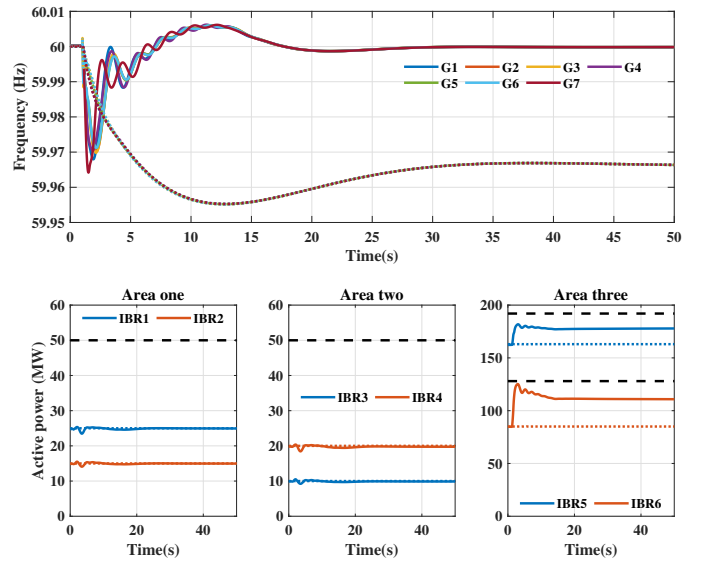


Fig. 3. Frequency and active power profiles during a 70MW-100Mvar load change; VC priority.

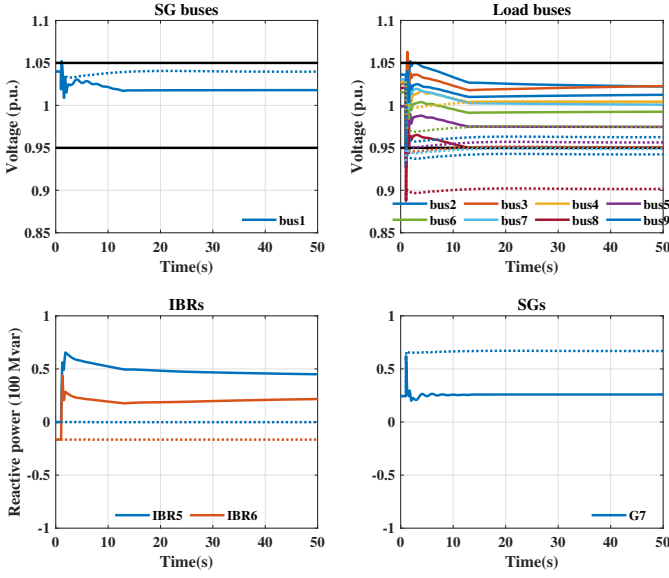


Fig. 4. Voltage and reactive power profiles in Area 3 during a 70MW-100Mvar load change; VC priority.

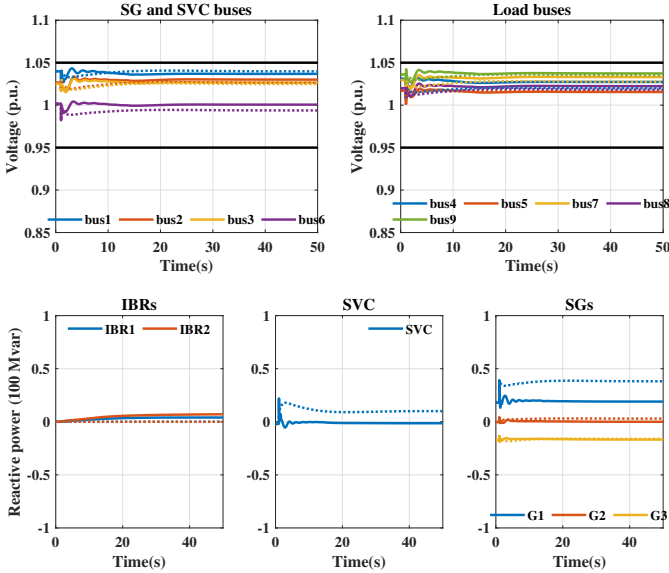


Fig. 5. Voltage and reactive power profiles in non-contingent areas during a 70MW-100Mvar load change; VC priority.

### B. Scenario # 2: severe load disturbance

This scenario examines the effect of a more severe load disturbance in the system and allows us to compare the performance of the two operational modes (Section III-A). In this scenario, a load disturbance of 150 MW and 80 MVar is introduced at  $t = 1$ s at bus 8 in Area 3.

The response of the system is shown in Fig. 6, 7 and 8 for the case where the VC has priority and in Fig. 9, 10 for the case where the FC has priority. Here, dotted and solid lines refer to cases without and with control, respectively; the dashed line refers to the control limit of each IBR. Improved voltage control performance is achieved when the control

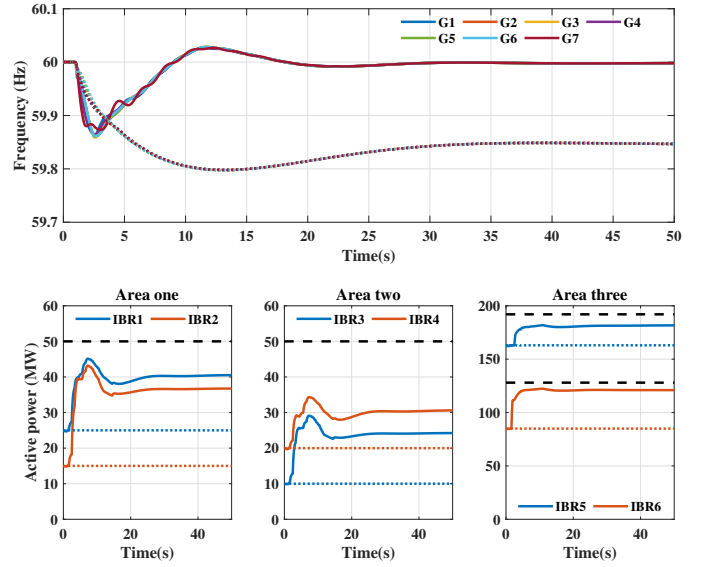


Fig. 6. Frequency and active power profiles during a 150MW-100Mvar load change; VC priority.

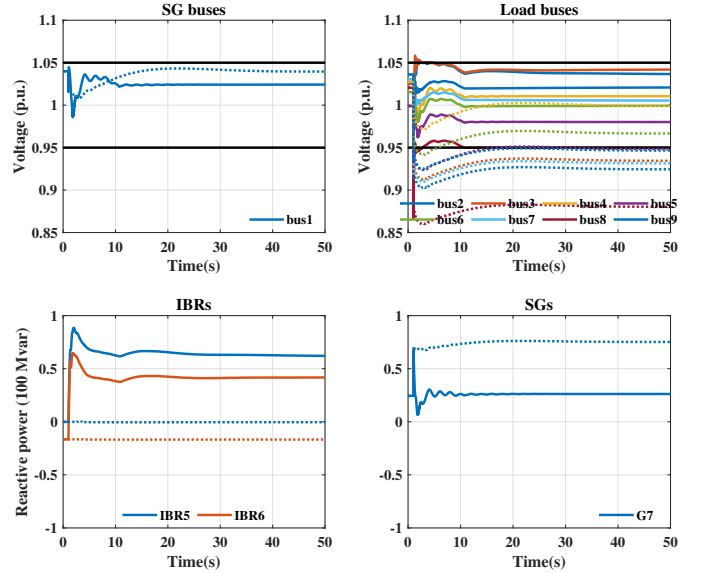


Fig. 7. Voltage and reactive power profiles in Area 3 during a 150MW-100Mvar load change; VC priority.

mode is set as  $VC > FC$  compared to  $FC > VC$ . Both control modes regulate the system frequency back to the nominal value. In both cases ( $FC$  or  $VC$  priority), the second stage of  $FC$  with support from neighbors is activated when the IBRs in the contingent area reach their maximum capacity. Although the frequency response is significantly better for  $FC > VC$  operational mode, it comes at the cost of voltage violations due to insufficient local reactive power capacity. This illustrates the inherent trade-off between the two operational modes.

Finally, the effect of the PSS-Controller interactions detailed in Section III-C can be clearly observed in Fig. 8, where the solid and dotted plots show the response with and without

low-pass filtering. All the PSSs installed in the test system utilized in this work are of the multi-band damping variety and one can clearly see the PSS signals and the VC's SGs setpoints opposing each other at the input to the SG excitation system. Adding a low-pass filter to the VC's SGs voltage setpoints command, as suggested in Section III-C, smooths the signal during most parts of the transient, with a gradual ramp towards its steady-state value. This idea is to ensure that the PSS signal dominates during the transient period, when it is most aggressive.

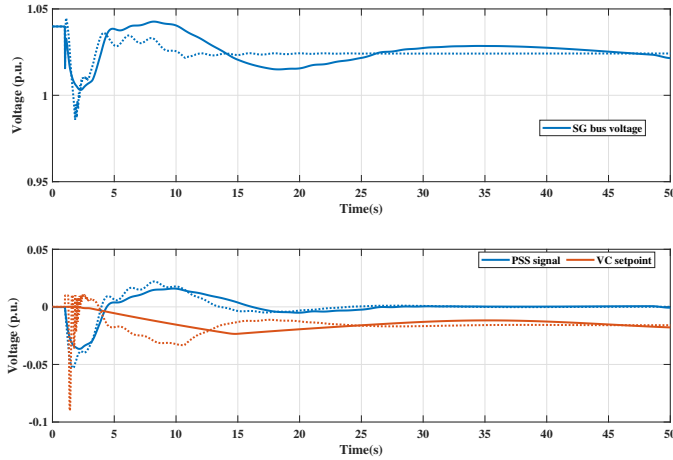


Fig. 8. SG and PSS signals during a 150MW-100Mvar load change; VC priority.

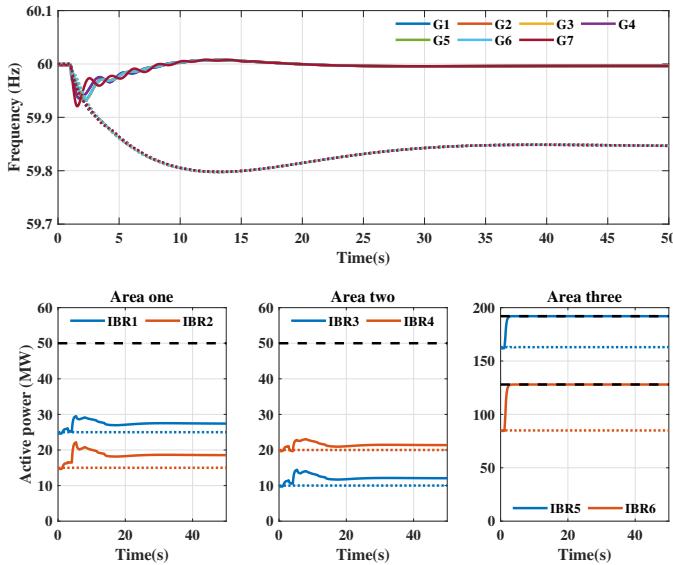


Fig. 9. Frequency and active power profiles during a 150MW-100Mvar load change; FC priority.

## V. CONCLUSION

This paper has detailed the integration of two novel frequency and voltage controllers designed previously in [5], [6] into a joint control framework. This integration allows both controllers to simultaneously utilize IBRs with minimum

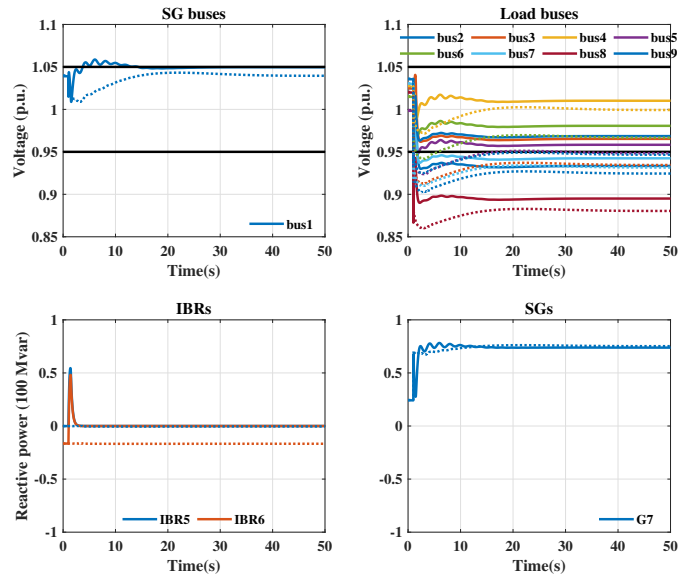


Fig. 10. Voltage and reactive power profiles in Area 3 during a 150MW-100Mvar load change; FC priority.

conflict and interaction. Simulation results have been presented to validate the approach and to highlight the trade-offs inherent in different operational modes. Future work is primarily concerned with data-driven extensions of the individual controller designs, and integration of the controllers with distribution-level resources.

## REFERENCES

- [1] IRENA, "Global energy transformation: A roadmap to 2050," 2018.
- [2] B. K. Poolla, S. Bolognani, and F. Dörfler, "Optimal placement of virtual inertia in power grids," *IEEE Trans. Autom. Control*, vol. 62, no. 12, pp. 6209–6220, 2017.
- [3] H. Sun, Q. Guo, J. Qi, V. Ajarapu, R. Bravo, J. Chow, Z. Li, R. Moghe, E. Nasr-Azadani, U. Tamrakar, *et al.*, "Review of challenges and research opportunities for voltage control in smart grids," *IEEE Trans. Power Syst.*, vol. 34, no. 4, pp. 2790–2801, 2019.
- [4] Q. Guo, H. Sun, B. Wang, B. Zhang, W. Wu, and L. Tang, "Hierarchical automatic voltage control for integration of large-scale wind power: Design and implementation," *Electric Power Syst. Research*, vol. 120, pp. 234–241, 2015.
- [5] E. Ekomwenrenren, Z. Tang, J. W. Simpson-Porco, E. Farantatos, M. Patel, and H. Hooshyar, "Hierarchical coordinated fast frequency control using inverter-based resources," *IEEE Trans. Power Syst.*, vol. 36, no. 6, pp. 4992–5005, 2021.
- [6] Z. Tang, E. Ekomwenrenren, J. W. Simpson-Porco, E. Farantatos, M. Patel, and H. Hooshyar, "Measurement-based fast coordinated voltage control for transmission grids," *IEEE Trans. Power Syst.*, vol. 36, no. 4, pp. 3416–3429, 2021.
- [7] M. Morari and E. Zafriou, *Robust process control*. Chemical Engineering Research and Design, Prentice Hall, 1987.
- [8] J. V. Milanovic, K. Yamashita, S. M. Villanueva, S. Ž. Djokic, and L. M. Korunović, "International industry practice on power system load modeling," *IEEE Trans. Power Syst.*, vol. 28, no. 3, pp. 3038–3046, 2012.
- [9] A. Khodabakhshian, M. E. Pour, and R. Hooshmand, "Design of a robust load frequency control using sequential quadratic programming technique," *International Journal of Electrical Power & Energy Systems*, vol. 40, no. 1, pp. 1–8, 2012.
- [10] A. Delavari, I. Kamwa, and P. Brunelle, "Simscape power systems benchmarks for education and research in power grid dynamics and control," in *IEEE Canadian Conf. on ECE*, pp. 1–5, 2018.